Manipulating polarization of light with ultrathin epsilon-near-zero metamaterials

P. Ginzburg,[1,*] F. J. Rodríguez Fortuño,[1,2] G. A. Wurtz,[1] W. Dickson,[1] A. Murphy,[3] F. Morgan,[3] R. J. Pollard,[3] I. Iorsh,[4] A. Atrashchenko,[4,5] P. A. Belov,[4] Y. S. Kivshar,[4,6] A. Nevet,[7] G. Ankonina,[7] M. Orenstein,[7] and A. V. Zayats[1]

[1]*Department of Physics, King's College London, Strand, London WC2R 2LS, UK*
[2]*Nanophotonics Technology Center. Universitat Politècnica de València. 46022 Valencia, Spain*
[3]*Centre for Nanostructured Media, The Queen's University of Belfast, Belfast, BT7 1NN, UK*
[4]*National Research University of Information Technologies, Mechanics and Optics (ITMO), St. Petersburg 197101, Russia*
[5]*Ioffe Physical-Technical Institute of the Russian Academy of Sciences, St. Petersburg 194021, Russia*
[6]*Nonlinear Physics Center and Centre for Ultrahigh Bandwidth Devices for Optical Systems (CUDOS) Research School of Physics and Engineering, The Australian National University, Canberra ACT 0200, Australia*
[7]*Electrical Engineering Department, Technion–Israel Institute of Technology, Technion City, Haifa 32000, Israel*
[*]*pavel.ginzburg@kcl.ac.uk*

Abstract: One of the basic functionalities of photonic devices is the ability to manipulate the polarization state of light. Polarization components are usually implemented using the retardation effect in natural birefringent crystals and, thus, have a bulky design. Here, we have demonstrated the polarization manipulation of light by employing a thin subwavelength slab of metamaterial with an extremely anisotropic effective permittivity tensor. Polarization properties of light incident on the metamaterial in the regime of hyperbolic, epsilon-near-zero, and conventional elliptic dispersions were compared. We have shown that both reflection from and transmission through λ/20 thick slab of the metamaterial may provide nearly complete linear-to-circular polarization conversion or 90° linear polarization rotation, not achievable with natural materials. Using ellipsometric measurements, we experimentally studied the polarization conversion properties of the metamaterial slab made of the plasmonic nanorod arrays in different dispersion regimes. We have also suggested all-optical ultrafast control of reflected or transmitted light polarization by employing metal nonlinearities.

OCIS codes: (240.6680) Surface plasmons; (350.4238) Nanophotonics and photonic crystals.

References and links

1. M. Born and E. Wolf, *Principles of Optics: Electromagnetic Theory of Propagation, Interference and Diffraction of Light* (Cambridge University, 2000).
2. A. K. Sarychev and V. M. Shalaev, *Electrodynamics of Metamaterials*, (World Scientific, 2007).
3. A. Papakostas, A. Potts, D. M. Bagnall, S. L. Prosvirnin, H. J. Coles, and N. I. Zheludev, "Optical manifestations of planar chirality," Phys. Rev. Lett. **90**(10), 107404 (2003).
4. M. Hentschel, M. Schäferling, T. Weiss, N. Liu, and H. Giessen, "Three-Dimensional chiral plasmonic oligomers," Nano Lett. **12**(5), 2542–2547 (2012).
5. C. Helgert, E. Pshenay-Severin, M. Falkner, C. Menzel, C. Rockstuhl, E. B. Kley, A. Tünnermann, F. Lederer, and T. Pertsch, "Chiral metamaterial composed of three-dimensional plasmonic nanostructures," Nano Lett. **11**(10), 4400–4404 (2011).
6. A. Drezet, C. Genet, J. Y. Laluet, and T. W. Ebbesen, "Optical chirality without optical activity: How surface plasmons give a twist to light," Opt. Express **16**(17), 12559–12570 (2008).
7. T. Ellenbogen, K. Seo, and K. B. Crozier, "Chromatic plasmonic polarizers for active visible color filtering and polarimetry," Nano Lett. **12**(2), 1026–1031 (2012).
8. Y. Zhao, M. A. Belkin, and A. Alù, "Twisted optical metamaterials for planarized ultrathin broadband circular polarizers," Nat. Commun. **3**, 870 (2012).

9. J. K. Gansel, M. Thiel, M. S. Rill, M. Decker, K. Bade, V. Saile, G. von Freymann, S. Linden, and M. Wegener, "Gold helix photonic metamaterial as broadband circular polarizer," Science **325**(5947), 1513–1515 (2009).
10. N. I. Zheludev, E. Plum, and V. A. Fedotov, "Metamaterial polarization spectral filter: isolated transmission line at any prescribed wavelength," Appl. Phys. Lett. **99**(17), 171915 (2011).
11. M. Atatüre, J. Dreiser, A. Badolato, and A. Imamoglu, "Observation of Faraday rotation from a single confined spin," Nat. Phys. **3**(2), 101–106 (2007).
12. I. Crassee, J. Levallois, A. L. Walter, M. Ostler, A. Bostwick, E. Rotenberg, T. Seyller, D. Marel, and A. B. Kuzmenko, "Giant Faraday rotation in single- and multilayer graphene," Nat. Phys. **7**(1), 48–51 (2011).
13. C. R. Simovski, P. A. Belov, A. V. Atrashchenko, and Y. S. Kivshar, "Wire metamaterials: physics and applications," Adv. Mater. **24**(31), 4229–4248 (2012).
14. G. A. Wurtz, R. Pollard, W. Hendren, G. P. Wiederrecht, D. J. Gosztola, V. A. Podolskiy, and A. V. Zayats, "Designed ultrafast optical nonlinearity in a plasmonic nanorod metamaterial enhanced by nonlocality," Nat. Nanotechnol. **6**(2), 107–111 (2011).
15. A. V. Kabashin, P. Evans, S. Pastkovsky, W. Hendren, G. A. Wurtz, R. Atkinson, R. Pollard, V. A. Podolskiy, and A. V. Zayats, "Plasmonic nanorod metamaterials for biosensing," Nat. Mater. **8**(11), 867–871 (2009).
16. V. A. Podolskiy and E. E. Narimanov, "Strongly anisotropic waveguide as a nonmagnetic left-handed system," Phys. Rev. B **71**(20), 201101 (2005).
17. P. Ginzburg and M. Orenstein, "Nonmetallic left-handed material based on negative-positive anisotropy in low-dimensional quantum structures," J. Appl. Phys. **103**(8), 083105 (2008).
18. P. Ginzburg and M. Orenstein, "Metal-free quantum-based metamaterial for surface plasmon polariton guiding with amplification," J. Appl. Phys. **104**(6), 063513 (2008).
19. C. L. Cortes, W. Newman, S. Molesky, and Z. Jacob, "Quantum nanophotonics using hyperbolic metamaterials," J. Opt. **14**(6), 063001 (2012).
20. A. N. Poddubny, P. A. Belov, P. Ginzburg, A. V. Zayats, and Y. S. Kivshar, "Microscopic model of Purcell enhancement in hyperbolic metamaterials," Phys. Rev. B **86**(3), 035148 (2012).
21. R. W. Ziolkowski, "Propagation in and scattering from a matched metamaterial having a zero index of refraction," Phys. Rev. E. **70**(4), 046608 (2004).
22. M. G. Silveirinha and N. Engheta, "Tunneling of electromagnetic energy through subwavelength channels and bends using epsilon-near-zero materials," Phys. Rev. Lett. **97**(15), 157403 (2006).
23. B. Edwards, A. Alù, M. E. Young, M. Silveirinha, and N. Engheta, "Experimental verification of ε-near-zero metamaterial coupling and energy squeezing using a microwave waveguide," Phys. Rev. Lett. **100**(3), 033903 (2008).
24. R. Liu, Q. Cheng, T. Hand, J. J. Mock, T. J. Cui, S. A. Cummer, and D. R. Smith, "Experimental demonstration of electromagnetic tunneling through an epsilon-near-zero metamaterial at microwave frequencies," Phys. Rev. Lett. **100**(2), 023903 (2008).
25. P. Ginzburg, A. Nevet, N. Berkovitch, A. Normatov, G. M. Lerman, A. Yanai, U. Levy, and M. Orenstein, "Plasmonic resonance effects for tandem receiving-transmitting nano-antennas," Nano Lett. **11**(1), 220–224 (2011).
26. A. Normatov, P. Ginzburg, N. Berkovitch, G. M. Lerman, A. Yanai, U. Levy, and M. Orenstein, "Efficient coupling and field enhancement for the nano-scale: plasmonic needle," Opt. Express **18**(13), 14079–14086 (2010).
27. R. Atkinson, W. R. Hendren, G. A. Wurtz, W. Dickson, A. V. Zayats, P. Evans, and R. J. Pollard, "Anisotropic optical properties of arrays of gold nanorods embedded in alumina," Phys. Rev. B **73**(23), 235402 (2006).
28. R. J. Pollard, A. Murphy, W. R. Hendren, P. R. Evans, R. Atkinson, G. A. Wurtz, A. V. Zayats, and V. A. Podolskiy, "Optical nonlocalities and additional waves in epsilon-near-zero metamaterials," Phys. Rev. Lett. **102**(12), 127405 (2009).
29. N. Liu, H. Liu, S. Zhu, and H. Giessen, "Stereometamaterials," Nat. Photonics **3**(3), 157–162 (2009).
30. P. Ginzburg, F. J. Rodríguez-Fortuño, A. Martínez, and A. V. Zayats, "Analogue of the quantum Hanle effect and polarization conversion in non-Hermitian plasmonic metamaterials," Nano Lett. **12**(12), 6309–6314 (2012).
31. M. Ren, E. Plum, J. Xu, and N. I. Zheludev, "Giant nonlinear optical activity in a plasmonic metamaterial," Nat. Commun. **3**, 833 (2012).
32. L. V. Alekseyev, E. E. Narimanov, T. Tumkur, H. Li, Yu. A. Barnakov, and M. A. Noginov, "Uniaxial epsilon-near-zero metamaterial for angular filtering and polarization control," Appl. Phys. Lett. **97**(13), 131107 (2010).
33. R. Kullock, W. R. Hendren, A. Hille, S. Grafström, P. R. Evans, R. J. Pollard, R. Atkinson, and L. M. Eng, "Polarization conversion through collective surface plasmons in metallic nanorod arrays," Opt. Express **16**(26), 21671–21681 (2008).
34. T. Li, S. M. Wang, J. X. Cao, H. Liu, and S. N. Zhu, "Cavity-involved plasmonic metamaterial for optical polarization conversion," Appl. Phys. Lett. **97**(26), 261113 (2010).
35. T. Li, H. Liu, S. Wang, X. Yin, F. Wang, S. N. Zhu, and X. Zhang, "Manipulating optical rotation in extraordinary transmission by hybrid plasmonic excitations," Appl. Phys. Lett. **93**(2), 021110 (2008).
36. J. Hao, Y. Yuan, L. Ran, T. Jiang, J. A. Kong, C. T. Chan, and L. Zhou, "Manipulating electromagnetic wave polarizations by anisotropic metamaterials," Phys. Rev. Lett. **99**(6), 063908 (2007).
37. P. Yeh, "Optics of anisotropic layered media: a new 4x4 matrix algebra," Surf. Sci. **96**(1-3), 41–53 (1980).
38. W. S. Chang, J. B. Lassiter, P. Swanglap, H. Sobhani, S. Khatua, P. Nordlander, N. J. Halas, and S. Link, "A plasmonic fano switch," Nano Lett. **12**(9), 4977–4982 (2012).

#184277 - $15.00 USD Received 28 Jan 2013; revised 19 Mar 2013; accepted 21 Mar 2013; published 17 Jun 2013

39. M. Kauranen and A. V. Zayats, “Nonlinear plasmonics,” Nat. Photonics **6**(11), 737–748 (2012).
40. J. Elser, R. Wangberg, V. A. Podolskiy, and E. Narimanov, “Nanowire metamaterials with extreme optical anisotropy,” Appl. Phys. Lett. **89**(26), 261102 (2006).

1. Introduction

The ability to manipulate the polarization of light is essential for numerous applications spanning tele- and data communications, spectroscopy and microscopy, to name a few. The most commonly used approach for polarization rotation and conversion is based on either half- and quarter-wave plates utilizing retardation effects in anisotropic crystals [1]. However, almost all natural birefringent materials have a small ratio between refractive indices associated with the different crystallographic directions, resulting in relatively thick retardation plates, typically more than tens of microns (dozens of wavelengths).

On the other hand, metamaterials provide an unprecedented opportunity to manipulate light in previously impossible ways and achieve peculiar refractive index properties [2]. In terms of polarization manipulation, optically active artificially structured media have been demonstrated in several configurations, e.g., planar arrays of subwavelength gammadions [3], chiral plasmonic structures [4, 5], spiral bull-eye grooves [6], chromatic plasmonic polarizers [7], and twisted nanorods stacks [8]. Efficient broadband [9] and narrowband polarizers [10] have also been demonstrated. Other novel approaches such as Faraday rotators based on single confined spin excitations [11] or graphene sheets [12], require either macroscopic designs or challenging technological efforts to achieve acceptable levels of reliability and repeatability.

Intrinsically anisotropic metamaterials having a high ratio between permittivity tensor components, such as those based on thin film layered structures or wire arrays, have recently attracted significant attention [13]. In particular, metamaterial composites based on plasmonic nanorods demonstrate an extremely high optical anisotropy that has already been employed in a number of very promising applications, such as ultrafast optical modulation [14] and sensing [15]. Extremely anisotropic metamaterials can exhibit properties of negative refraction [16, 17] and gain [18], hyperbolic dispersion in certain frequency ranges [19, 20], epsilon-near-zero (ENZ) behavior, and peculiar linear and nonlinear optical responses related to the aforementioned properties. In the conceptually different epsilon-near-zero regime [21], the metamaterial is supporting truly quasistatic excitations for high frequency electromagnetic fields which accumulate zero phase delays while propagating through such an assembly. For example, ENZ materials have been proposed for extraordinary transmission stability in bent structures [22] and experimentally demonstrated employing a number of approaches [23, 24].

In this paper, we demonstrate efficient manipulation of polarization properties of light using a metamaterial slab based on plasmonic nanorods. We compare polarization properties of reflected and transmitted light in the regimes of hyperbolic, ENZ and conventional dispersion and show the experimental proof of concept for a functional polarization converter based on a plasmonic nanorod metamaterial slab. Wavelength-dependent control over polarization was demonstrated in passive regime, and an active device has been proposed by employing the intrinsic nonlinearities of metal.

2. Results and discussion

A plasmonic metamaterial consisting of arrays of vertically aligned and electromagnetically coupled Au nanorods is an example of a highly anisotropic artificial medium [Fig. 1(a)]. Having properties different of those of isolated rods [25, 26], it can be described by the diagonal permittivity tensor in the effective medium approximation (see Methods):

$$\ddot{\varepsilon} = \begin{pmatrix} \varepsilon_{\parallel} & & \\ & \varepsilon_{\parallel} & \\ & & \varepsilon_{\perp} \end{pmatrix}, \tag{1}$$

where $\varepsilon_{\parallel}$ is the permittivity for the electric field perpendicular to the nanorod axes (parallel to the metamaterial layer), while $\varepsilon_{\perp}$ is the permittivity for the electric field parallel to the nanorod axes (normal to the metamaterial layer) [27]. Due to the plasmonic nature of the optical response of metal, the $\varepsilon_{\perp}$ component may become negative in the long wavelength range of the spectrum for certain geometrical parameters of the nanorod array. Anisotropic metamaterials with permittivity components having opposite signs, namely, $\varepsilon_{\perp}\varepsilon_{\parallel} < 0$, are called hyperbolic metamaterials, since they have hyperbolic isofrequency contours. The elliptic dispersion requires $\varepsilon_{\perp}\varepsilon_{\parallel} > 0$, while the ENZ regime is achieved for $\varepsilon_{\perp}\varepsilon_{\parallel} \approx 0$ with, as a rule of thumb, $n_{eff,\perp} < 1$. The advanced fabrication techniques enable control over the length, diameter and periodicity of the nanorods and, hence, allow tuning of the ENZ frequency to the desired values required for a particular application [27]. By engineering the anisotropy of the artificial metamaterial, precise control over the polarization of light can be achieved using simple reflection or transmission configurations with a sub-wavelength thick metamaterial slab [Fig. 1(b)].

To illustrate anisotropic properties of nanorod metamaterial, we first consider a typical nanorod metamaterial, which will be used in the subsequent ellipsometric measurements. The metamaterial consisting of 350 nm height Au nanorods with 30 nm diameter and 60 nm average spacing between nanorods, embedded in alumina, can be attributed the real and imaginary parts of the effective permittivity components $\varepsilon_{\perp}$ and $\varepsilon_{\parallel}$ shown in Fig. 1(c). The effective permittivities were derived using the effective medium theory (see Methods for details), neglecting nonlocal spatial dispersion effects. The hyperbolic dispersion regime interfaces the conventional elliptical one at a wavelength of around 735 nm at which the ENZ regime occurs. In the elliptical regime (wavelengths shorter 735 nm), the anisotropy of metamaterial is very strong with the ordinary and extraordinary refraction index difference $\mathrm{Re}(n_{\parallel}) - \mathrm{Re}(n_{\perp}) \approx 0.25$ at $\lambda = 500$ nm, comparable to the anisotropy achievable with naturally available anisotropic crystals such as rutile ($\Delta n = 0.3$). At the same time, losses are significant in this spectral range, also introducing significant dichroism ($\Delta k = 0.04$). In the hyperbolic regime, the index difference is $\mathrm{Re}(n_{\parallel}) - \mathrm{Re}(n_{\perp}) \approx 1.44$ at $\lambda = 1$ μm which exceeds the anisotropy of all naturally occurring crystals. With the remarkable reduction of the losses for the field component perpendicular to the nanorod axes, the linear dichroism effect is further increased ($\Delta k = 1.7$). Thus, the metamaterials provide record values for anisotropy and birefringence, which can be engineered by controlling structural parameters or indeed dynamically with active control of the optical properties of metamaterial constituents by external stimuli.

#184277 - $15.00 USD Received 28 Jan 2013; revised 19 Mar 2013; accepted 21 Mar 2013; published 17 Jun 2013

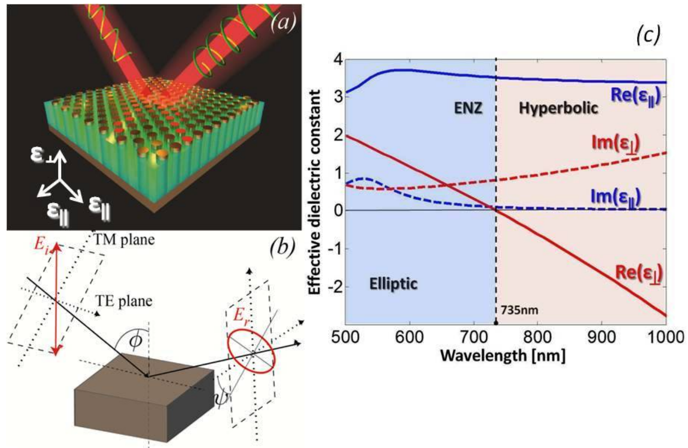

Fig. 1. (a) Schematic view of the plasmonic nanorod metamaterial layer for polarization control in reflection or transmission. (b) Geometry and definitions for elipsometric parameters. (c) Real (red) and imaginary (blue) parts of the effective permittivity tensor components $\varepsilon_\perp$ and $\varepsilon_\parallel$ of the metamaterial. The metamaterial consists of Au nanorods deposited within aluminium oxide matrix, nanorod height and diameter are 350 nm and 30 nm, respectively, nanorod spacing is 60 nm. Spectral ranges of elliptic and hyperbolic dispersions are also indicated.

2.1. Polarization conversion in a nanorod metamaterial

To determine the anisotropy required for linear polarization rotation by 90° (the effect of half-waveplate) or conversion of linear to circular polarization (the effect of quarter-waveplate), the dependence of the reflection and transmission parameters were studied as the function of the anisotropy strength, the metamaterial slab thickness, and angle of incidence (the polarization conversion does not occur at normal incidence since TE and TM waves are degenerate in the case of uniaxial anisotropy). One permittivity component (Re($\varepsilon_\perp$)) was varied while keeping the other fixed $\varepsilon_\parallel = 4 + 0.1i$. Initially, the material losses Im($\varepsilon_\perp$) = 0.1 were introduced in order to remove the effect of dichroism which is related to different absorption of different polarization components and prevent non-physical phase fluctuations close to the ENZ point (in the absence of losses, the effect of nonlocal spatial dispersion effects [28] can significantly influence the results).

The metamaterial parameters required to achieve specific polarization conversion of the linearly (p-) polarized incident light can be inferred from Fig. 2 where red-dashed curves correspond to the phase shift of $\Delta = \pi/2$ between the TE and TM components of the electric field [Fig. 1(b)], demanded for circular polarization, while blue-doted curves satisfies the phase of $\Delta = \pi$, required for rotation of polarization plane, and green-solid curves for the amplitude ratios of 1. The intersections (marked with black crosses) of red and green curves satisfy the conditions of the complete conversion of the linear polarization into circular one, the blue and green curves intersections correspond to 90° rotation of the incident linear polarization – both upon reflection [Figs. 2(a), 2(b)] or transmission [Figs. 2(c), 2(d)]. All other points on these parametric maps lead to elliptical polarization. As can be seen from Fig. 2, polarization conversion occurs in the vicinity of the ENZ point, even with very thin metamaterial layers of a fraction of λ thickness. In all considered cases, 'half-waveplate' and 'quarter-waveplate' effects occur for refractive indexes much less than 1, emphasizing the role of the ENZ regime. Comparable performance may only be achieved with much thicker components based on natural materials. For example, rutile (TiO_2) crystal has an extremely high natural anisotropy of about 10%, resulting in a quarter-wave plate of 514 nm thickness at the wavelength of 590 nm.

#184277 - $15.00 USD Received 28 Jan 2013; revised 19 Mar 2013; accepted 21 Mar 2013; published 17 Jun 2013

Generally, strong rotation capability is observed close to ENZ point in both cases of weak hyperbolic and elliptic dispersions, providing huge polarization rotations angles – as high as 1000-3000 [°/λ], while for natural crystals (e.g., rutile) this value does not exceed 100 [°/λ]. The benefit of operating close to the ENZ regime relies on the fact that certain field components (perpendicular to the layer) are not accumulating propagation phase, while others do. In this scenario, it is easy to obtain sufficient phase differences over thin metamaterial layers. Subsequent increase of the layer thickness will introduce unequal losses in TE and TM components and break the balance between their amplitudes due to dichroism effects.

Beyond the parameters shown on the parametric maps in Fig. 2(a-d), the rest of the amplitude-phase space of the reflection scheme is presented in the 3D plots in Fig. 2(e,f) showing the dependences of ellipsometric angles [Eq. (4)] on the metamaterial layer thickness d/λ and $\mathrm{Re}(\varepsilon_\perp)$ at the angle of incidence of 60°. As expected, maximal phase accumulation occurs near the ENZ point, and a wide dynamic range of phase angles can be accumulated with deep-subwavelength metamaterial layers.

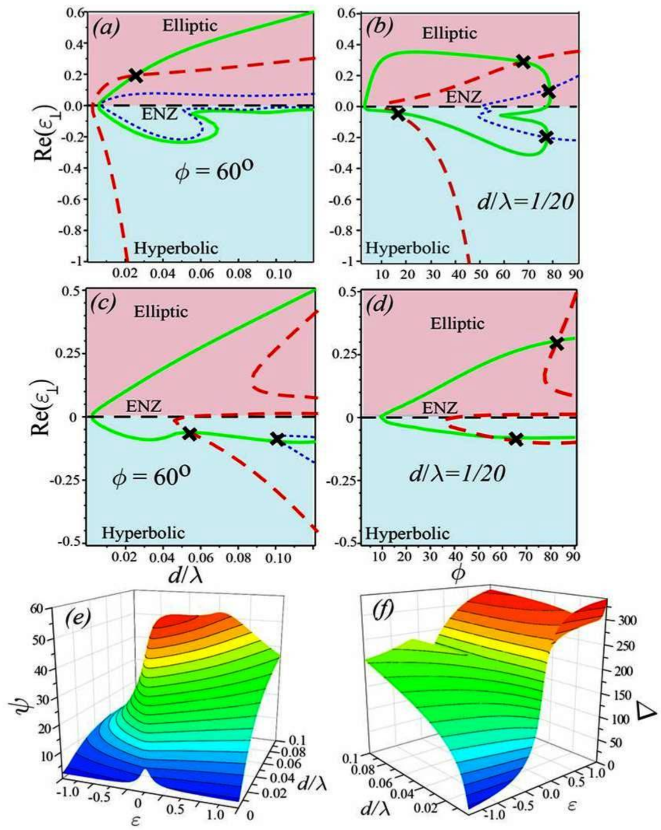

Fig. 2. Parametric plots for polarization conversion of p-polarized incident light in (a,b) reflection and (c,d) transmission configurations: red-dashed curves correspond $\Delta = \pi/2$, blue-doted curves to $\Delta = \pi$, green-solid curves to $|\xi| = 1$. The linearly polarized light is incident from the air side. (a,c) The angle of incidence is $\varphi = 60°$. (b,d) The thickness is $d = \lambda/20$. Metamaterial parameters are: $\varepsilon_\parallel = 4 + 0.1i$ and $\mathrm{Im}(\varepsilon_\perp) = 0.1$. Black crosses are the intersections corresponding to conversion to circular polarization (red-green lines intersection) and to 90° linear polarization rotation (blue-green lines intersection). (e,f) 3D plots of Ψ and Δ ellipsometric parameters (in degrees) for reflected light as the function of layer thickness d/λ and $\mathrm{Re}(\varepsilon_\perp)$. The incident light is p-polarized. The angle of incidence is 60°. Spectral ranges of elliptic and hyperbolic dispersions are also indicated.

#184277 - $15.00 USD Received 28 Jan 2013; revised 19 Mar 2013; accepted 21 Mar 2013; published 17 Jun 2013

The discussed manipulation of light polarization with a plasmonic nanorod metamaterial has several advantages over others recently demonstrated, both in performance and fabrication simplicity. Other proposed approaches for polarization control with metamaterials include the use of stereometamaterials [29] and twisted [8] metamaterial that serve as very efficient polarizers but require much more complicated layer-by-layer fabrication and hundreds of nanometers separation between the layers. Helix metamaterial based devices are also of micron thickness [9]. ‘Nonhermitian’ metamaterials promise remarkable performances even with very thin single layers [30]. Nonlinear optical activity in metamaterials could be millions times higher than in natural crystals but, being power dependent, is small compared with linear polarization changes [31]. It has to be noted that nanorods-based ENZ metamaterials have been shown to act as polarizers and narrowband angular transmittance filters [32] but not as polarization converters. Arrays of gold nanorods were also tested in terms of polarization state change in the transmission regime, but they have not been considered as a platform for on demand polarization control [33]. Similarly, L-shaped hole arrays in a metal film can be used for efficient polarization rotation in transmission [34, 35]. Metamaterials have been also proposed to design polarization control functionalities in microwave spectral range [36].

2.2. Experimental realization

The spectral dependence of extinction, reflection and ellipsometric angles Ψ and Δ, extracted from measurements described in ‘Methods’, provide confirmation of the predicted strong polarization effects [Figs. 3(a)-3(f)]. The experiments were performed for five different angles of incidence in the range from 35° to 55°. The extinction spectra [Fig. 3(a)] extracted from the transmission measurements, are typical of the plasmonic nanorod metamaterials with the transverse resonance at around 520 nm excited with light having an electric field component normal to the nanorod axes and the longitudinal resonance at around 700 nm excited by light polarized parallel to the nanorod axes. With the increase of the angle of incidence, the longitudinal resonance become more pronounced as the component of the electric field along the nanorod axes increases. The longitudinal peak is situated near the ENZ wavelength as has been observed previously [27]. The reflection spectra have complex structure with less pronounced angular dependencies [Fig. 3(c)]. The longitudinal resonance of the extinction spectra can be correlated to the reduced reflection.

The measured parameter Δ which describes polarization plane rotation, varies significantly when the transition from conventional to hyperbolic dispersion regime occurs [Figs. 3(e), 3(f)]. It can be seen that there exists a set of frequencies for which Δ is equal to 90° indicating full conversion from linear to circular polarization in reflection. The 90° point is very sensitive to the angle of incidence and could be obtained in the vicinity of the ENZ regime. On the other hand, ψ, the measure of amplitude change, is close to 45° throughout the whole spectral range showing that the linear dichroism of the structure plays a minor role for the thin structures under investigation.

The experimental data have been modelled using analytical expressions obtained from the transfer matrix technique [37] with the effective permittivities shown in Fig. 1(c). For these metamaterial parameters, the absolute value of ratio of $\varepsilon_{\perp}$ and $\varepsilon_{\parallel}$ does not exceed 1, which is similar to the conditions assumed for the dependences in Fig. 2. It can be seen that the spectral dependences, as well as the absolute values of all parameters in Fig. 3 are well described by the theoretical model. The optimal geometrical parameters for the fitting are within 5% of those directly measured from the fabricated structure (see Methods).

#184277 - $15.00 USD Received 28 Jan 2013; revised 19 Mar 2013; accepted 21 Mar 2013; published 17 Jun 2013

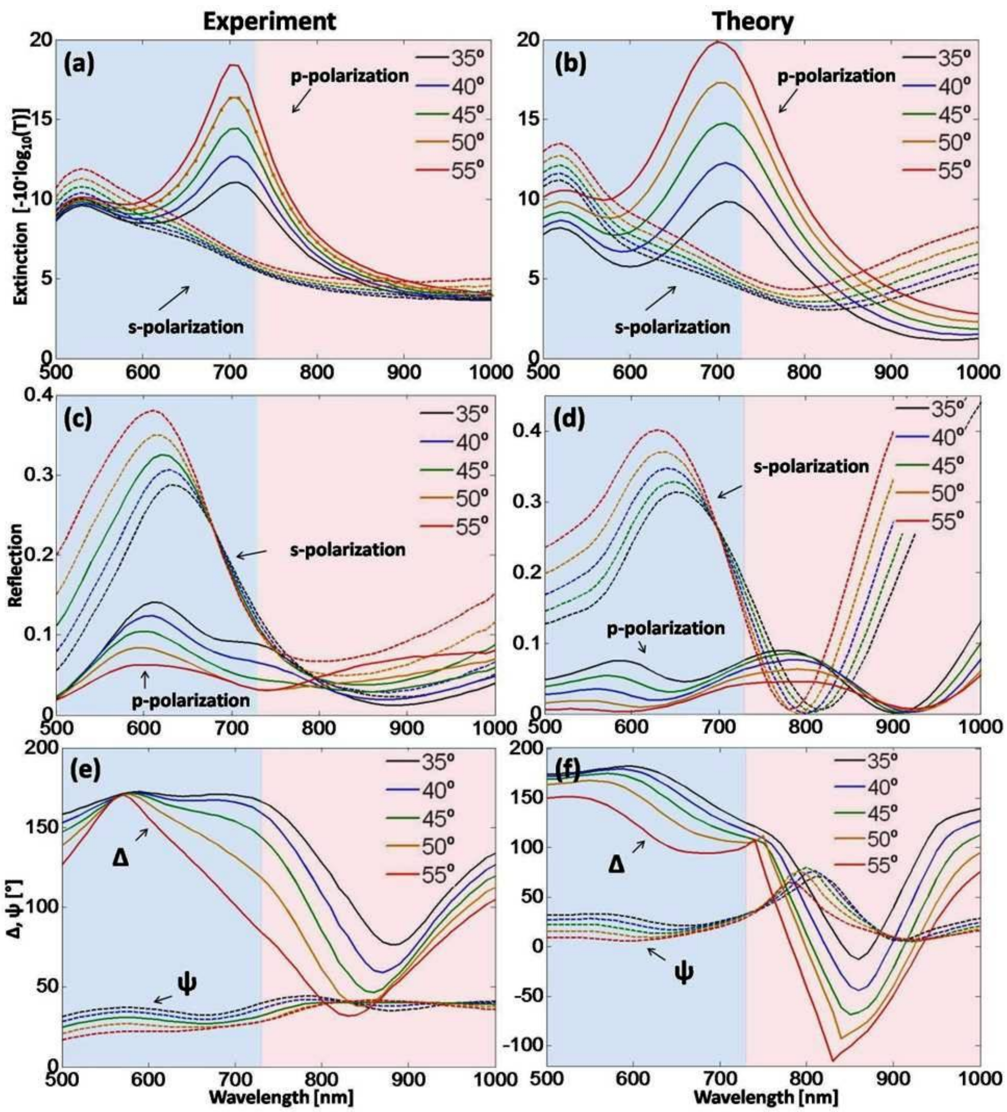

Fig. 3. (a,c,e) Experimental and (b,d,f) theoretical spectra of (a,b) extinction and (c,d) reflection for p-polarized (solid lines) and s-polarized (dashed lines) light for different incidence angles. (e,f) The spectra of ellipsometric parameters Δ (solid lines) and Ψ (dashed lines) for different incidence angles. Metamaterial parameters are as in Fig. 1(c). Spectral ranges of elliptic and hyperbolic dispersions are also indicated.

The strongest deviations between experiment and modeling are observed for polarization parameters plots, since the polarization, i.e., phase sensitive measurements are much more sensitive to small variations in sample parameters than the intensity measurements of reflection and transmission. In particular, the modeled behavior of Δ shows abrupt changes (with a discontinuous derivative) close to the ENZ point [Fig. 3(f)] where the field components perpendicular to the metamaterial layer have 'π' shift in phase. Near the wavelength where the reflection is very close to zero a strong variation in phase is also observed, as should be expected. At the same time, in the experimentally measured dependences, the minimum reflection is further from zero, thus the Δ variations are smaller. The primary origin for the deviations between the experiment and the model for all of the reported results is related to imperfections of the sample, especially the non-uniformities in nanorod height. While spatial dispersion (nonlocal effects) were not taken into account and, in general, expected to have a little influence in the un-annealed nanorod metamaterials due to losses, the high sensitivity of polarization measurements may still be able to 'see' them, leading to additional deviations between the theory and experiment.

2.3. All-optical control of polarization

Plasmonic nanostructures provide an interesting opportunity to achieve active plasmonic components [14, 38, 39]. In this context, we have investigated the possibility of controlling the polarization conversion all-optically by employing intrinsic metal nonlinearity introduced by free electron heating [14]. This nonlinearity involves both inter- and intraband electron transitions and may be observed in short-pulse pump-probe experiments, benefiting from the fast dynamics of collective nonradiative relaxation processes in electron plasma. It has recently been demonstrated that such nonlinearity can lead to fast (THz-speeds) and strong (up to 80% change in transmission) modifications of the optical response of metal nanorod metamaterials [14] as well as split-ring-based metamaterials [30]. While in the previous work ultrafast transmission changes (intensity modulation) were demonstrated, here we propose the ultrafast modulation of phase which leads to changes in polarization of reflected or transmitted light.

Figure 4 shows the modelled changes of Ψ and Δ parameters in the reflection configuration as the function of the electron temperature in the nanorods, induced by the pump beam. The results show that the polarization can be modulated very substantially on the sub-picosecond time scale. The considered signal wavelengths of 635, 735, and 835 nm were chosen to be in the region of elliptic, ENZ, and hyperbolic dispersion, respectively. The most pronounced modulation is observed close to the ENZ and weak hyperbolic regimes where the phase changes manifest themselves in the most pronounced way.

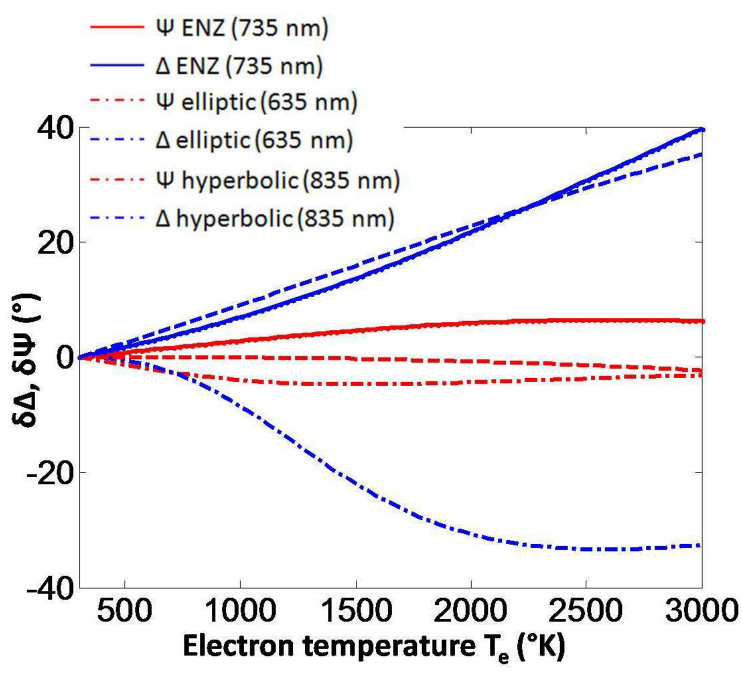

Fig. 4. All-optical control of polarization conversion in the metamaterial upon reflection for different wavelengths: the dependences of (blue lines) rotation angle Δ and (red lines) amplitude angle ψ on the electron temperature in Au nanorods. Metamaterial parameters are as in Fig. 1(c). The metamaterial layer thickness is $d/\lambda = 1/20$ and the angle of incidence is $\varphi = 60°$

#184277 - $15.00 USD Received 28 Jan 2013; revised 19 Mar 2013; accepted 21 Mar 2013; published 17 Jun 2013

3. Conclusions

We have proposed and experimentally demonstrated ultrathin nanorod metamaterial based components for manipulation of light polarization. Both reflection and transmission configurations have been experimentally shown to provide linear-to-circular polarization conversion in a 350 nm thick slab at oblique incidence, which cannot be achieved by employing any naturally existing material in geometries of similar simplicity and which typically require components of tens of microns thickness, based on natural uniaxial crystals. Theoretically, complete linear-to-circular polarization conversion or 90° linear polarization rotation in both reflection from and transmission through a λ/20 thick slab of metamaterial can be achieved. Moreover, ultrafast all-optical phase modulation of the reflected and transmitted light can be achieved leading to significant (about 40° rotation) changes of polarization state of the signal light. This is an important step towards ultrasensitive polarization devices for free-space and integrated photonics as well as active devices for ultrafast, low-power, all-optical information processing on the deep-subwavelength scale utilizing electron nonlinearities of metamaterial components.

4. Methods

Polarization properties modeling. Considering a slab of a uniaxial anisotropic material with a principal axis oriented perpendicularly to a transparent isotropic substrate and bounded by vacuum [Fig. 1(b)], the reflection coefficients for p-polarized (TM) and s-polarized (TE) modes can be expressed as

$$r_p = \frac{\left(1 - k_{z,sub} / \left(\varepsilon_{sub} k_{0z}\right)\right) - i\tan\left(k_{zp} d\right)\left(\varepsilon_{\parallel} k_{z,sub} / \left(\varepsilon_{sub} k_{zp}\right) - k_{zp} / \left(\varepsilon_{\parallel} k_{zp}\right)\right)}{\left(1 + k_{z,sub} / \left(\varepsilon_{sub} k_{0z}\right)\right) - i\tan\left(k_{zp} d\right)\left(\varepsilon_{\parallel} k_{z,sub} / \left(\varepsilon_{sub} k_{zp}\right) + k_{zp} / \left(\varepsilon_{\parallel} k_{zp}\right)\right)} \tag{2}$$

and

$$r_s = \frac{\left(1 - k_{z,sub} / \left(\varepsilon_{sub} k_{0z}\right)\right) - i\tan\left(k_{zs} d\right)\left(\varepsilon_{\parallel} k_{z,sub} / \left(\varepsilon_{sub} k_{zs}\right) - k_{zs} / \left(\varepsilon_{\parallel} k_{zp}\right)\right)}{\left(1 + k_{z,sub} / \left(\varepsilon_{sub} k_{0z}\right)\right) - i\tan\left(k_{zs} d\right)\left(\varepsilon_{\parallel} k_{z,sub} / \left(\varepsilon_{sub} k_{zs}\right) + k_{zs} / \left(\varepsilon_{\parallel} k_{zp}\right)\right)}, \tag{3}$$

respectively. Here, $k_{zp}^2 = \varepsilon_{\parallel} k_0^2 - \beta^2 \varepsilon_{\parallel} / \varepsilon_{\perp}, k_{zs}^2 = \varepsilon_{\parallel} k_0^2 - \beta^2$, $k_{z,sub}^2 = \varepsilon_{sub} k_0^2 - \beta^2$, and $k_{0z}^2 = k_0^2 - \beta^2$; β is the in-plane (xy) component of the wavevector of the incident light, d is the thickness of the metamaterial slab; $\varepsilon_{\parallel}$ and $\varepsilon_{\perp}$ are the components of the metamaterial dielectric permittivity tensor (Eq. (1), respectively, ε_{sub} is the dielectric permittivity of the substrate, while the superstrate was assumed to be vacuum $\varepsilon_{\sup} = 1$.

The polarization changes experienced by a plane wave reflected from a planar surface are derived from the ratio of the reflection coefficients (r_p / r_s) for its p- (TM) and s- (TE) polarized components (Fig. 1) and in general is a complex number [1]:

$$\xi = \frac{r_p}{r_s} = \tan(\psi) e^{i\Delta}, \tag{4}$$

where ψ is the measure of the amplitude ratio and Δ represents the phase rotation. The polarization conversion of the incident beam from linear polarization into circular one corresponds to $\xi = i$ ($\psi = 45^\circ, \Delta = 90^\circ$), while $\xi = -1$ ($\psi = 45^\circ, \Delta = 180^\circ$) corresponds to the polarization rotation by 90°.

Effective medium model. In order to model the optical properties of the metamaterial, the experimental parameters of the nanorods were used to calculate the dielectric permittivity of the layer by applying the standard Maxwell-Garnett effective medium model presented in [40] with a modified intra-rod interaction tensor γ.

Sample fabrication. The metamaterial sample fabrication sequence, similar to the one described in [14], involves the reactive magnetron sputter deposition of a 10 nm thick Tantalum pentoxide adhesion layer on a 1 mm thick glass substrate, followed by the deposition of a 5 nm thick gold electrode with a 350 nm thick aluminum layer on top. The latter is then anodized in sulphuric acid (20 V) to obtain a nanoporous alumina template in which gold nanorods are electrochemically grown. The metamaterials studied here is made of rods with 350 nm height, 30 nm diameter, and 60 nm average interrod spacing.

Experimental measurements. The ellipsometric measurements have been performed using J. A. Woollam Co. commercial instrument. The reflection and transmission spectra in the range of angle of incidence and in the various polarization configurations (s-s, s-p, p-p, p-s) were recorded with both amplitude and phase information. The amplitude ratio and phase rotation have then been derived.

Acknowledgments

This work has been supported in part by EPSRC (UK) and ERC. P. G. acknowledges support from the Royal Society via the Newton International Fellowship.